NASA TECHNICAL MEMORANDUM

NASA TM X-68102

NASA TM X-68102

FORWARD FLIGHT EFFECTS ON MIXER NOZZLE DESIGN AND NOISE CONSIDERATIONS FOR STOL EXTERNALLY BLOWN FLAP SYSTEMS

by U. von Glahn, N. Sekas, D. Groesbeck and R. Huff
Lewis Research Center
Cleveland, Ohio

TECHNICAL PAPER proposed for presentation at
Fourth Aircraft Design Flight Test and Operation Meeting
sponsored by the American Institute of Aeronautics and Astronautics
Los Angeles, California, August 7-9, 1972

FORWARD FLIGHT EFFECTS ON MIXER NOZZLE DESIGN AND NOISE CONSIDERATIONS FOR STOL EXTERNALLY BLOWN FLAP SYSTEMS

U. von Glahn*, N. Sekas, D. Groesbeck and R. Huff

National Aeronautics and Space Administration
Lewis Research Center
Cleveland, Ohio 44135

Abstract

Experimental data of the peak axial-velocity decay in a moving airstream are presented for several types of nozzles. The nozzles include a six-tube mixer nozzle of a type considered for reduction of jet-flap interaction noise for externally-blown-flap STOL aircraft. The effect of secondary flow on the core flow velocity decay of a bypass nozzle is also discussed. Tentative correlation equations are suggested for the configurations evaluated. Recommendations for minimizing forward velocity effects on velocity decay and jet-flap interaction noise are made.

E-7028

Nomenclature

(All nomenclature in English units)

C_n - effective nozzle coefficient

D_e - effective diameter of nozzle or single element

D_x - displacement parameter (defined in ref. 5)

M_o - free stream Mach number

M_j - jet exhaust Mach number

U - peak velocity

U_c - core exhaust velocity

U_j - jet exhaust velocity

U_ℓ - local velocity

U_o - free stream velocity

U_s - secondary exhaust velocity

X - axial distance downstream of nozzle exhaust plane

$Z_{(1)}$ - departure point of coalescing core decay curve from single element decay curve

Introduction

Externally blown flaps (EBF) have been proposed as one means of lift augmentation for STOL aircraft (fig. 1). Studies have shown that the jet impingement on the deflected flaps during approach or takeoff can cause an unacceptable increase in the aircraft noise signature. The increase in noise is approximately a six-power function of the impinging jet velocity and the flap and wing surface area scrubbed by the jet. [1, 2] The jet-flap interaction noise can be lowered by reducing the impinging jet velocity through the use of mixer-type nozzles. [3] Such nozzles consist of multi-elements rather than a single large exhaust nozzle of equal total area. The individual elements of a mixer nozzle promote mixing of the jet with the surrounding air resulting in a rapid axial velocity decay. [4, 5, 6]

It has been demonstrated in the literature that the rate of velocity decay for a jet from a single circular nozzle is reduced when the jet is surrounded by a moving airstream. [7, 8] Because a reduced velocity decay could result in an increase in jet-flap interaction noise during takeoff and landing for an EBF STOL airplane, a study was initiated to determine the effect of forward velocity on a typical mixer nozzle.

This paper summarizes the results of an experimental study conducted at the NASA Lewis Research Center on the peak axial-velocity decay obtained with a single convergent circular nozzle and a six-tube mixer nozzle in a moving airstream. Empirical equations are developed for estimating peak axial-velocity decay curves for a wide range of operating conditions.

Recommendations are made regarding mixer nozzle design points for minimizing forward velocity effects on the velocity decay and hence jet-flap interaction noise.

Apparatus

The aerodynamic studies were conducted in a Lewis 6- by 9-foot subsonic wind tunnel [9] at tunnel-air velocities up to 400 ft/sec. The nozzles were mounted in the tunnel test section on a streamlined pod as shown in Fig. 2. The center portion of the pod served as a plenum in the nozzle airflow system.

Pressurized air at about 520° R is supplied to the model nozzle through a strut and the plenum. Airflow through the supply line was measured with a calibrated orifice. The nominal nozzle inlet total pressure was measured with a single probe near the plenum exit flange. Jet surveys at various downstream locations from the nozzle exit plane were made initially with a rake consisting of pitot and static tubes (fig. 2). Pressures were recorded from mercury and water manometer boards.

Later in the program the rake was replaced with a

*Chief, Jet Acoustics Branch, Member AIAA.

traversing pitot-static tube. Surveys again were made at various downstream locations from the nozzle exit plane. The pressures measured with the pitot-static probe were transmitted to an x-y-y' plotter which yielded direct traces on graph paper of the total and static pressure distribution across the jet and adjacent tunnel airstream.

In addition, the static test stand described in Ref. 5 was used for some configurations.

Configurations

Velocity decay data in a moving airstream were obtained with a single, convergent circular nozzle (fig. 3(a)) and a six-tube mixer nozzle (fig. 3(b)). The single circular nozzle had a diameter of 2.28-in. which was equivalent in exhaust area to that for the six-tube nozzle.

The six-tube mixer nozzle was similar to a nozzle previously reported in Ref. 5 in which static test data are presented. This nozzle consisted of nominal 1-in. tubes (0.93-in. I.D.) each 6.2-in. long and spaced circumferentially 1-in. apart. A faired centerbody was used as shown in Fig. 3(b) to provide a reasonably good flow field between the tubes and minimize separation and recirculation flow in this region.

In addition, as shown in Fig. 3(c), an available 4.75 aspect-ratio slot nozzle (0.9-in. by 4.05-in., with rounded ends) surrounded by an annular nozzle (5.8-in. O.D. and 4.5-in. I.D.) was tested to evaluate the effect of secondary flow on a core flow from a single nozzle. The exhaust plane of the bypass nozzle was 5.5 in. upstream of the core exhaust plane. This nozzle was tested only on the static test stand described in Ref. 5. Screens were used ahead of the annular flow exhaust plane to vary the ratio of secondary- to core-flow.

Peak Velocity Decay

Single Circular Nozzle

The peak velocity decay of the single, convergent circular nozzle used as a reference herein is shown in Fig. 4 for various ratios of free stream Mach number to jet exhaust Mach number, M_o/M_j. (All symbols are defined in the nomenclature.) The data are shown in terms of the peak velocity decay U/U_j as a function of a dimensionless axial distance parameter, (5, 6) $X(C_n D_e\sqrt{1+M_j})^{-1}$. Also shown in the figure is a calculated velocity decay curve developed in Ref. 5 for a static condition, $M_o = 0$.

With increasing forward velocity, denoted by larger ratios of M_o/M_j, the data deviate increasingly more from the calculated static decay curve. The data curves (dashed lines) asymptotically approach a U/U_j value equal to U_o/U_j at large values of the distance (abscissa) parameter. It is apparent from this figure that with increasing forward velocity, the velocity decay ratio U/U_j (hence the peak velocity) downstream of the jet exhaust plane increases for a fixed value of X/D_e.

The literature(7, 8) suggests the use of a delta velocity ratio for normalizing the peak velocity decay of simple jets surrounded by a moving airstream. This dynamic or delta velocity ratio is given as $U-U_o/U_j-U_o$, where $U-U_o$ is the excess centerline or peak velocity over the free stream velocity.

In Fig. 5 the present jet decay data are shown in terms of the delta peak velocity ratio, $U-U_o/U_j-U_o$, as a function of $X(C_n D_e\sqrt{1+M_j})^{-1}$ for the same M_o/M_j values given in Fig. 4. Good correlation of the dynamic velocity decay data with the calculated static curve ($M_o = 0$) is noted for M_o/M_j values up to about 0.2. For M_o/M_j values greater than 0.2 the dynamic data increasingly deviate from the static curve with increasing M_o/M_j ratios.

In order to obtain a prediction procedure for large values of M_o/M_j, an exponent that is a function of M_o/M_j is required for the $X(C_n D_e\sqrt{1+M_j})^{-1}$ parameter. Such an exponent, b, was developed empirically and is given by:

$$b = 1 + 1/3\left[(U_j/U_o)^2 - 1\right]^{-1} \qquad (1)$$

The dynamic peak velocity decay data in terms of $U-U_o/U_j-U_o$ as a function of $\left[X(C_n D_e\sqrt{1+M_j})^{-1}\right]^b$ are shown in Fig. 6. Good correlation is achieved for nearly all of the data. It is believed that the deviations at the larger M_o/M_j values, shown in the lower right hand side of the figure, are caused by a complex interaction of the moving airstream with the reduced velocity of the jet stream, the wakes from the support structure and the nacelle boat-tail flow separation effects.

Mixer Nozzles

Background. - For multi-element nozzles in static conditions ($M_o = 0$), the initial peak axial-velocity decay, shown in Fig. 7, is substantially the same as that for an individual element. However, at some distance downstream of the nozzle exit plane, the individual jets coalesce sufficiently to form a large diameter coalescing core and a very slow peak-velocity decay occurs. Once the coalesced core has fully formed, normal mixing again occurs with an associated rapid velocity decay. It was determined (5, 6) that the axial decay distance for multi-element nozzles could be nondimensionalized for correlation purposes by the use of an effective diameter, D_e, based on that of a single element.

Empirical equations were developed to correlate the peak axial-velocity decay of multi-element nozzles in terms of the significant flow regimes shown in Fig. 7 and in terms of pertinent nozzle dimension parameters. (5, 6) These equations are limited, in general, to the nozzle geometries tested; however, they are useful in predicting the decay curves for many practical nozzle configurations.

In order to accomplish these predictions, the decay curve was divided into several regions shown in Fig. 8. Equations were then developed to predict the departure point of the coalescing core from the single-element

decay curve (point ①). Examination of the data showed that the velocity ratio in the coalescing core decay region had a slope of -0.2 with respect to axial distance (region denoted by ① to ②). The nondimensional displacement parameter, D_x, of the coalesced-core decay curve from the single-element curve was then determined. The value of U/U_j at point ② was then correlated in terms of the coalescing core decay slope and the displacement distance D_x. Finally, the correlation equation for the decay curve of the fully coalesced core was established.

Static condition, $M_o = 0$. - The peak velocity decay data for the present six-tube mixer nozzle is compared to that used in Ref. 5 in Fig. 9 for nominally static conditions. In general, the results are similar except at large values of X/D_e. The velocity decay in the coalescing core region for the present nozzle is substantially zero compared with a -0.2 slope for the data in Ref. 5. The change in the slope (from -0.2 to approximately zero) is attributed to the centerbody boat tail of the present nozzle; the previous nozzle used no centerbody. This effect of a nozzle centerbody also was observed with other nozzles.[4]

The coalescing region also extended farther downstream with the present nozzle than with that used in Ref. 5. This effect is believed due to the induced air velocity in the wind tunnel (up to approximately 40 ft/sec) caused by the ejector action of the nozzle.

Dynamic condition, $M_o > 0$. - The peak velocity decay data for the mixer nozzle with forward velocity are shown in Fig. 10 in terms of U/U_j as a function of $X(C_n D_e\sqrt{1+M_j})^{-1}$. Also shown is the calculated velocity decay curve[5] for the static condition ($M_o = 0$). In general, the trend with forward velocity for the mixer nozzle is similar to that for the single circular nozzle. With increasing M_o/M_j values, the ratio U/U_j increases at a fixed X/D_e value. The most significant difference between the two nozzles is that the asymptotic approach of the decay curve to a limiting U/U_j equal to U_o/U_j is delayed for the mixer nozzle by the coalescing core region.

The experimental decay data are shown in Fig. 11 in terms of the delta velocity decay parameter $U-U_o/U_j-U_o$ as a function of $X(C_n D_e\sqrt{1+M_j})^{-1}$. Again the trends are similar to those for the single convergent nozzle (fig. 5).

Correlation of the mixer nozzle peak velocity decay data is shown in Fig. 12 in which $U-U_o/U_j-U_o$ is plotted as a function of $[X(C_n D_e\sqrt{1+M_j})^{-1}]^b$. The exponent b is the same as that used for the single circular nozzle. It is apparent that good correlation is achieved in the region in which the jets act as single elements.

In the coalescing core region, the departure point from the single element curve is located at increasingly larger values of the abscissa parameter (fig. 12) with increasing values of M_o/M_j. A simple empirical equation was developed to predict the movement of the departure point, denoted as $Z_{①}$ in Ref. 6, with forward velocity as follows:

$$(Z_{①})_{dynamic} = (Z_{①})_{static}\left[\left(1 - \frac{U_o}{U_j}\right)\right]^{-1.25} \quad (2)$$

The static $Z_{①}$ value is calculated from equations given in Ref. 6. The calculated dynamic $Z_{①}$ values are shown by the arrows in Fig. 12. The dash lines in the figure represent the coalescing core region decay curves and were drawn parallel to the static curve.

Utilizing the preceding procedures and correlation techniques it would appear that the exhaust peak velocity decay curves in a moving airstream for EBF-STOL applications can be established to a satisfactory level.

Bypass nozzle. - For static conditions ($M_o = 0$), a bypass nozzle is a special case of the more general case of a core jet in a moving airstream. With a bypass nozzle the secondary jet flow constitutes a moving airstream for the core jet. The specialty of this case is that the secondary flow velocity as well as the core velocity decays with axial distance downstream of the exhaust planes of the two jets.

A plot of the peak velocity ratio for the bypass nozzle (fig. 3(c)) is shown in Fig. 13(a) as a function of $X(C_n D_e\sqrt{1+M_j})^{-1}$ for several ratios of secondary-to-primary exhaust velocities, U_s/U_c. The effect of the secondary flow is to shift the decay curves increasingly to right with increasing U_s/U_c values. The limited data shown with secondary flow can be normalized by dividing the $X(C_n D_e\sqrt{1+M_j})^{-1}$ parameter by $(1 + U_s/U_j)$ as shown in Fig. 13(b). It is apparent that the data with the secondary flows used do not correlate with the slot-nozzle-only data. The data with secondary flow follow a velocity decay curve characteristic of a circular nozzle rather than that of a slot nozzle.[6] This trend is attributed to the relatively high-velocity annular secondary flow. At very low values of U_s/U_c the decay curve can be expected to approach that for the slot nozzle.

Overall Jet Width

In the estimation of jet-flap interaction noise, the primary factor is the jet velocity; however, the area of the jet is also a significant factor. In particular, for the EBF-STOL aircraft, the jet impingement area on the flap is an important noise parameter. This impingement area is related directly to the overall jet size or width at the flap location.

Single circular nozzle. - Examination of the radial velocity profiles at various distances downstream of the single circular nozzle indicated only a slight effect of forward velocity on jet width for the range of M_o/M_j values applicable to EBF. In general, the profiles showed substantially no effect due to forward velocity at X/D_e values less than 10 and slightly decreased jet widths at larger X/D_e values.

Mixer nozzle. - In contrast to the single circular nozzle, the mixer nozzle overall jet width increased with forward velocity.

Because the departure point of the coalescing core from the single element decay curve is an important aerodynamic and acoustic design point, as will be discussed later, typical radial velocity profiles at this general location are shown in Fig. 14. The velocity profile data are presented in terms of the ratio of the local velocity to the jet exhaust velocity, U_ℓ/U_j, as a function of radial distance measured from the overall nozzle centerline. The data selected are for a static condition ($M_o = 0$) and free stream Mach number of 0.125. It is evident that the jet width increases with forward velocity. It appears that, because the jet velocity decay is decreased due to forward velocity, the individual jets maintain their identity and integrity for a longer distance downstream of the exhaust plane. Consequently, the outer boundary of the overall jet from the mixer nozzle is also maintained compared to jets operating in static conditions. It is also possible that the wake from the mixer nozzle boat-tail may have an effect on whether or not the jet width is larger or smaller with forward vleocity compared with the static case.

Application to EBF Noise

Propulsion systems for EBF-STOL airplanes can be grossly grouped into three categories: (1) low bypass engines with a bypass ratio of about six and an exhaust velocity between 850 and 1200 ft/sec, (2) high bypass engines with a bypass ratio of about 15 and an exhaust velocity near 650 ft/sec and (3) a fan-prop engine with a bypass ratio near 25 and an exhaust velocity near 450 ft/sec. The takeoff velocity for such aircraft using any of these propulsion systems is about 80 knots.

In order to estimate the change in jet-flap interaction noise due to forward velocity effects on jet velocity decay for these propulsion systems, it is assumed that a six-tube mixer nozzle of the type described herein is required. Furthermore, it is assumed that jet-flap interaction noise is a function only of the jet velocity impinging on the flap and the effective overall size of the jet ($U_\ell/U = 0.75$) at the flap location. This implies that jet-flap scrubbing noise is independent of relative velocity effects between impinging jet and the moving airstream.

The resulting peak velocity decay curves for the three types of propulsion systems using the six-tube mixer nozzle are shown in Fig. 15. The curves shown were calculated on the basis of the equations developed herein and those in Refs. 5 and 6. Velocity decay curves are shown for both the static condition and that at a free stream Mach number of about 0.12 (80 knots).

The departure points (knees in the curves), denoted by the circle and square symbols, represent optimum design points for the mixer nozzle used. The optimum design point for the use of a mixer nozzle with an EBF is defined as the least number elements (of a given cross sectional shape) to achieve a given U/U_j value with a minimum overall nozzle diameter at a given flap location (X/D_e). These criteria are met at the departure point of the coalescing core curve from the single element curve. Thus, the static design U/U_j for each propulsion system is 0.41 and occurs near an X/D_e of 20.

For the static design points (circle symbols), the effect of forward velocity is to increase the impingement velocity at any X/D_e including the flap location (X/D_e near 20, fig. 15). The largest increase in U/U_j occurs for the fan-prop engine (bypass ratio, 25) which has the largest M_o/M_j value (0.3). Furthermore, due to the greater jet width with forward velocity noted in Fig. 14, the impingement area at the flap location is assumed to become larger in a like manner. In estimating the jet-flap interaction noise with forward velocity, the jet outer boundary width at $U_\ell/U = 0.75$ was used to calculate the increased impingement area. A summary of the increase in noise level due to these effects of forward velocity on the jet exhaust characteristics is given for design point A in the following table:

Propulsion system	Increase in noise level over static condition, dB		
	Velocity increase	Area increase	Total
Low bypass	4.6	1	5.6
High bypass	6.3	1	7.1
Fan-prop	8.5	1	9.5

In order to avoid a noise increase with a mixer nozzle in flight, the design point of the dynamic decay curve (point B, square symbols in fig. 15) can be selected. In the present example, this yields a different U/U_j at the design point for each propulsion system application and an X/D_e near 25. It is evident from Fig. 15 that all forward velocities less than the takeoff velocity, including the static condition, the noise level would be less than that for the dynamic design point.

For design point B similar total noise changes to those obtained for design point A are obtained; however, the components that make up the noise increase are different and the changes are noise reductions rather than increases as in the case of design point A. The following table summarizes the change in noise level between design point B and the static condition for an X/D_e of 25.

Propulsion system	Decrease in noise level below forward velocity condition, dB		
	Velocity decrease	Area decrease	Total
Low bypass	-2.7	-3	-5.7
High bypass	-4.3	-3	-4.6
Fan-prop	-6.2	-3	-9.2

Concluding Remarks

On the basis of the noise estimates made herein, it is evident that a mixer nozzle design should be based on the peak velocity decay in a moving airstream (forward flight) in order to achieve a specified noise level; the latter being associated with a specific U/U_j value at the flap location. The noise level at static conditions for such a mixer nozzle design would be lower than that for the design flight condition.

With a single convergent circular nozzle, the jet-

flap interaction noise appears to be substantially independent of forward velocity since the X/D_e for such an installation is generally less than 10 and hence the U/U_j values and jet widths are not significantly affected by forward velocity.

References

1. Dorsch, R. G., Krejsa, E. A., and Olsen, W. A., "Blown Flap Noise Research," Paper 71-745, June 1971, AIAA, New York, N.Y.

2. Dorsch, R. G., Kreim, W. J., and Olsen, W. A., "Externally-Blown-Flap Noise," Paper 72-129, Jan. 1972, AIAA, New York, N.Y.

3. Goodykoontz, J. H., Dorsch, R. G., and Groesbeck, D. E., "Mixer Nozzle-Externally Blown Flap Noise Tests," TM X-68021, 1972, NASA, Cleveland, Ohio.

4. Groesbeck, D., Huff, R., and von Glahn, U.: "Peak Axial-Velocity Decay With Mixer-Type Exhaust Nozzle," TM X-67934, 1971, NASA, Cleveland, Ohio.

5. von Glahn, U. H., Groesbeck, D. E., and Huff, R. G., "Peak Axial-Velocity Decay With Single- and Multi-Element Nozzles," Paper 72-48, Jan. 1972, AIAA, New York, N.Y.

6. Groesbeck, D. E., von Glahn, U. H., and Huff, R. G., "Peak Axial-Velocity Decay With Multi-Element Rectangular and Triangular Nozzles," TM X-68047, 1972, NASA, Cleveland, Ohio.

7. Landis, F., and Shapiro, A. S., "The Turbulent Mixing of Co-Axial Gas Jets," Proceedings of the Heat Transfer and Fluid Mechanics Institute, Stanford Univ. Press, 1951, pp. 133-146.

8. Forstall, W., Jr., and Shapiro, A. H., "Momentum and Mass Transfer in Co-Axial Gas Jets," Journal of Applied Mechanics, Vol. 17, No. 4, Dec. 1950, pp. 399-408.

9. von Glahn, U. H., "The Icing Problem: Current Status of NACA Techniques and Research," Ottawa AGARD Conference, AGARD AG19/P9, 1955, pp. 293-331.

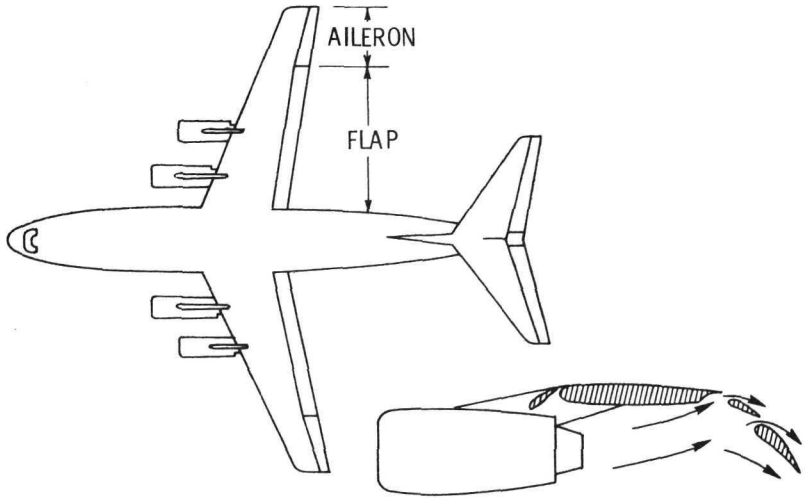

Figure 1. - Externally-blown-flap STOL airplane.

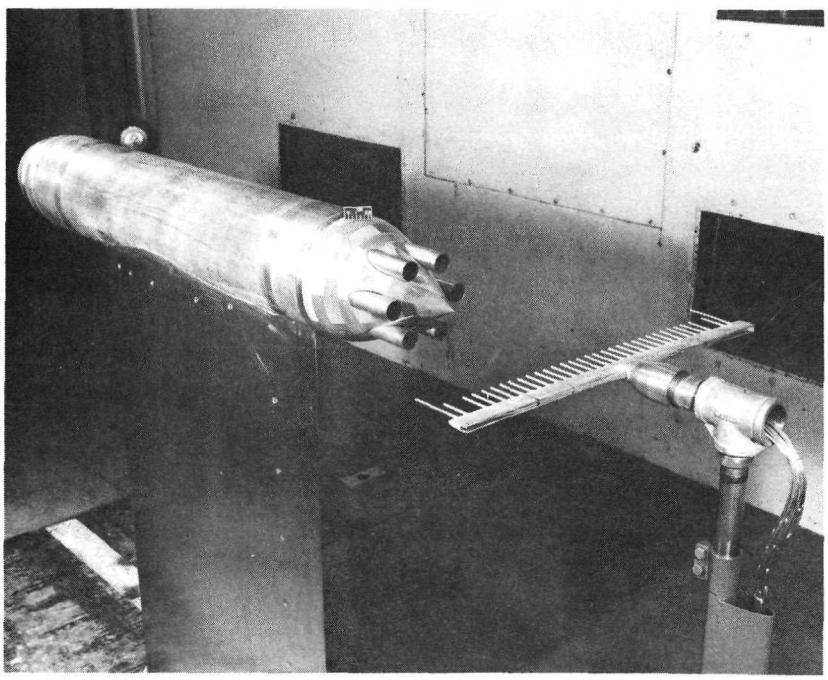

C-72-806

Figure 2. - 6-tube mixer nozzle installed in 6 x 9 foot wind tunnel.

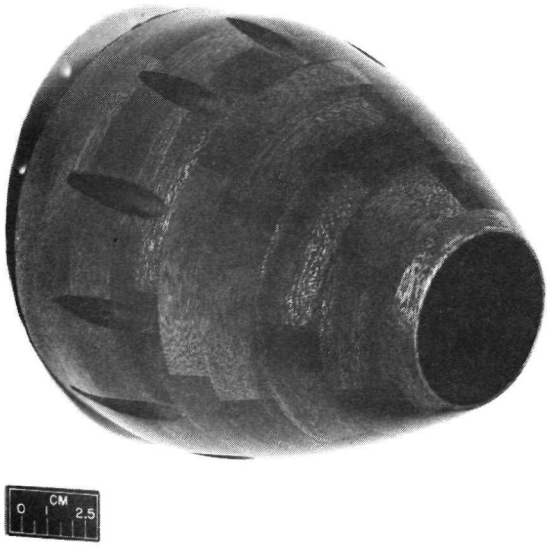

C-72-637

(a) SINGLE CONVERGENT CIRCULAR NOZZLE.

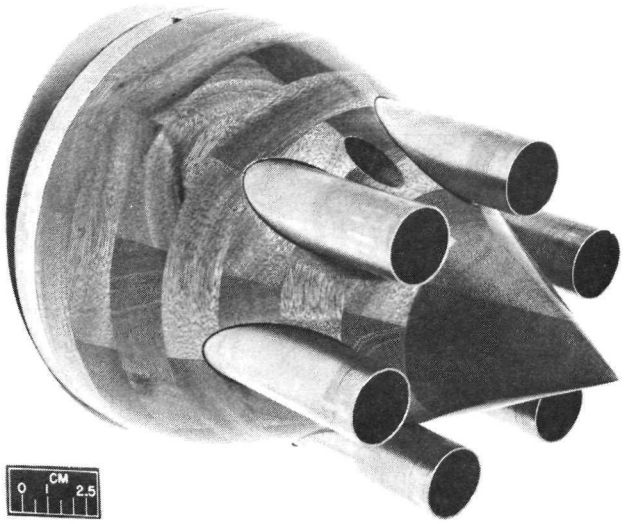

C-72-638

(b) 6-TUBE MIXER NOZZLE.

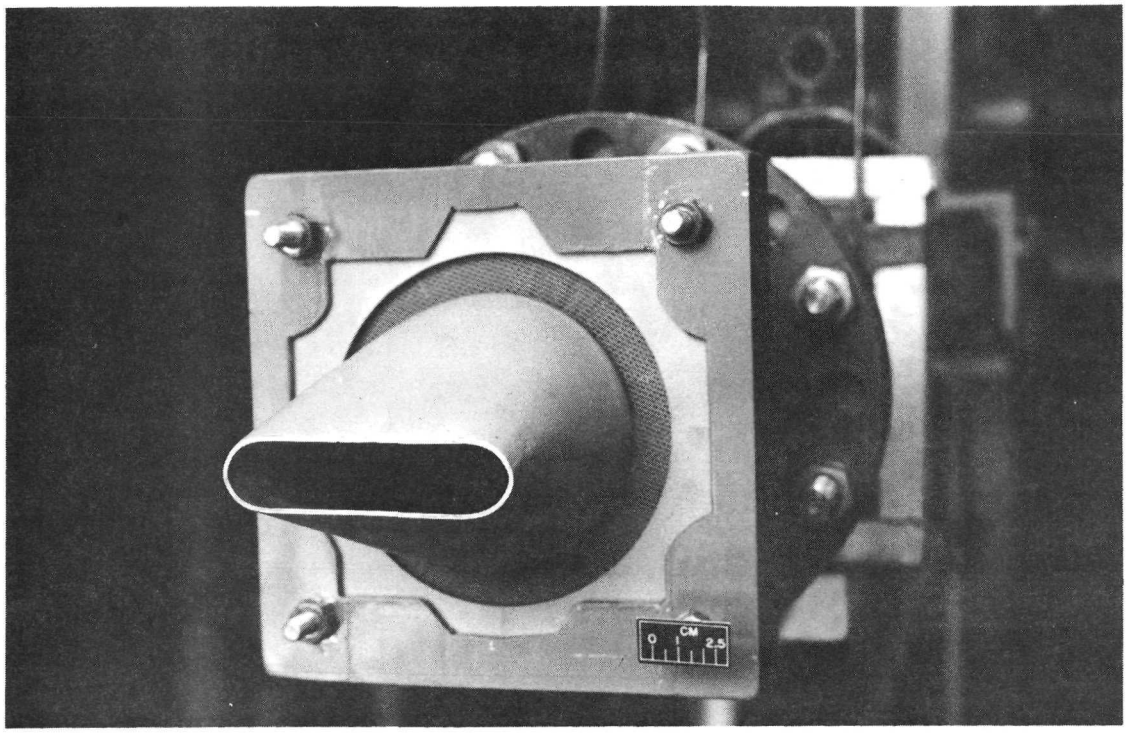

C-72-1418

(c) BYPASS-TYPE NOZZLE.

Figure 3. - Test nozzles.

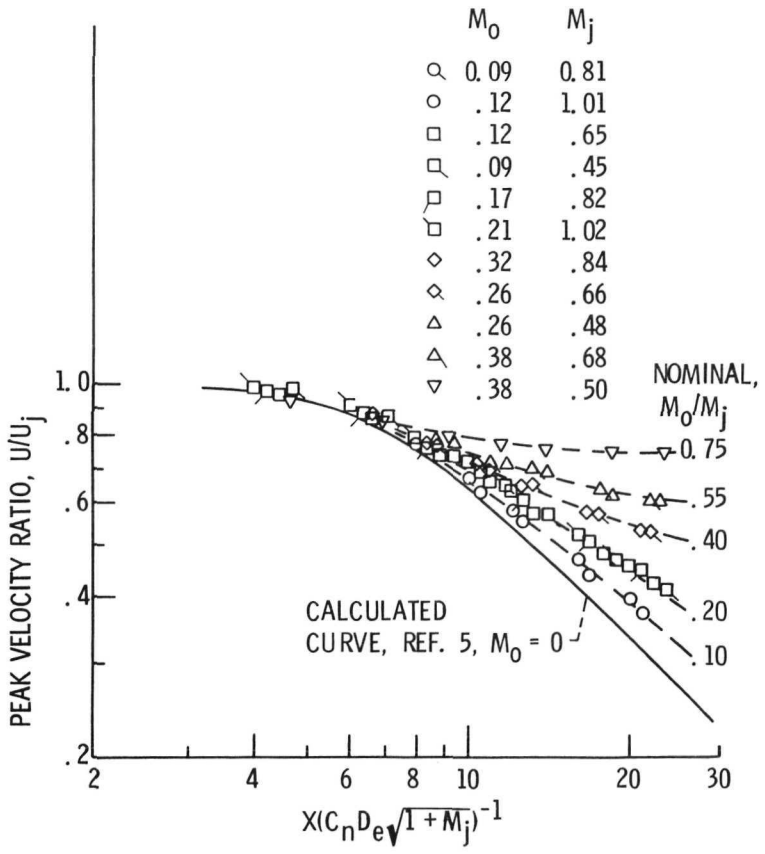

Figure 4. - Velocity decay for single circular nozzle. C_n, 0.77.

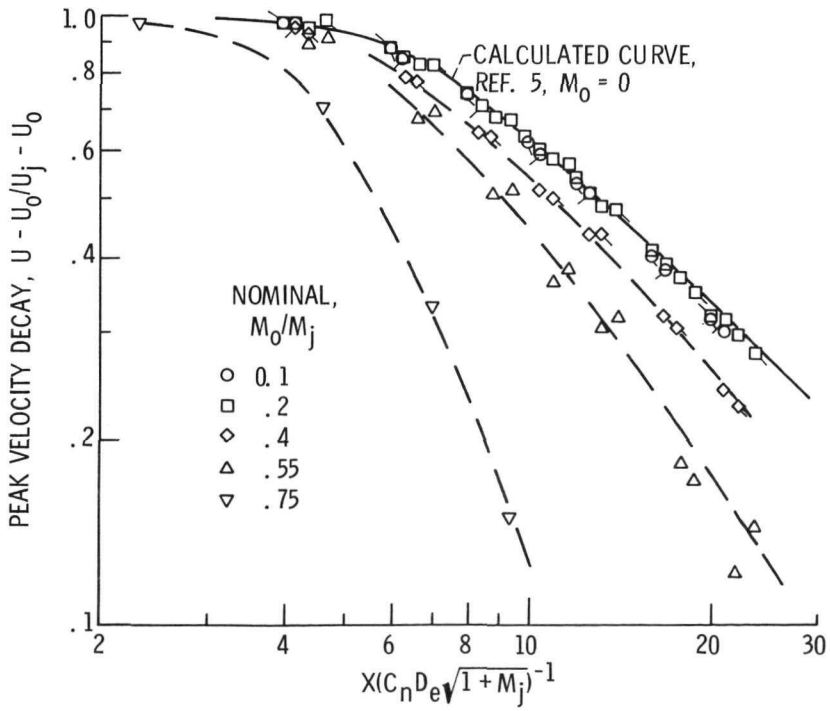

Figure 5. - Delta velocity decay for single circular nozzle.

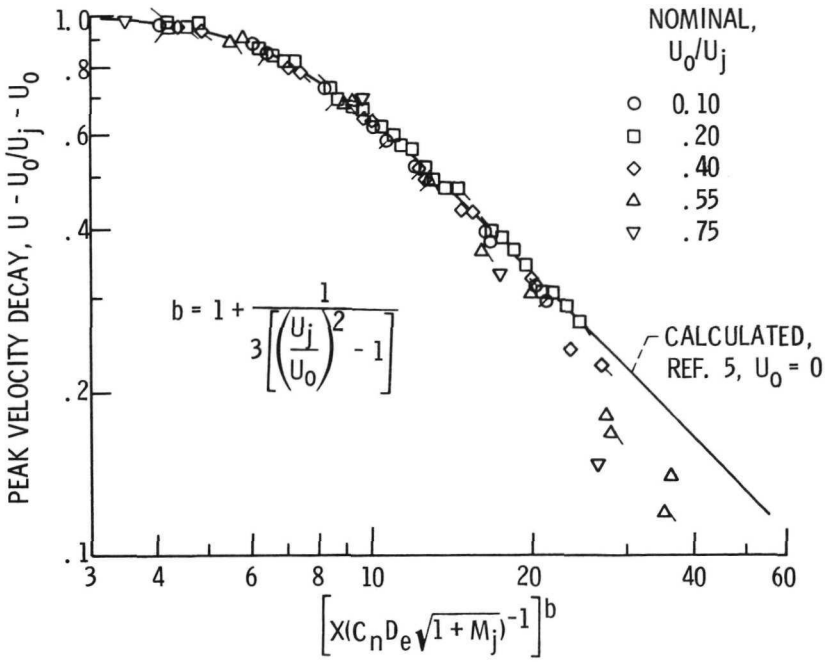

Figure 6. - Correlation of delta velocity decay for single circular nozzle.

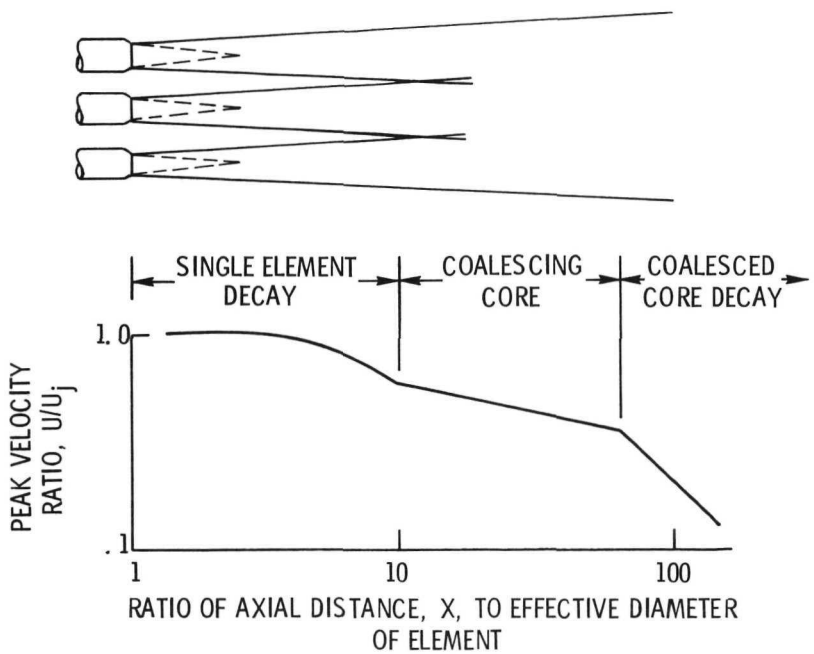

Figure 7. - Schematic of multi-element nozzle peak axial-velocity decay.

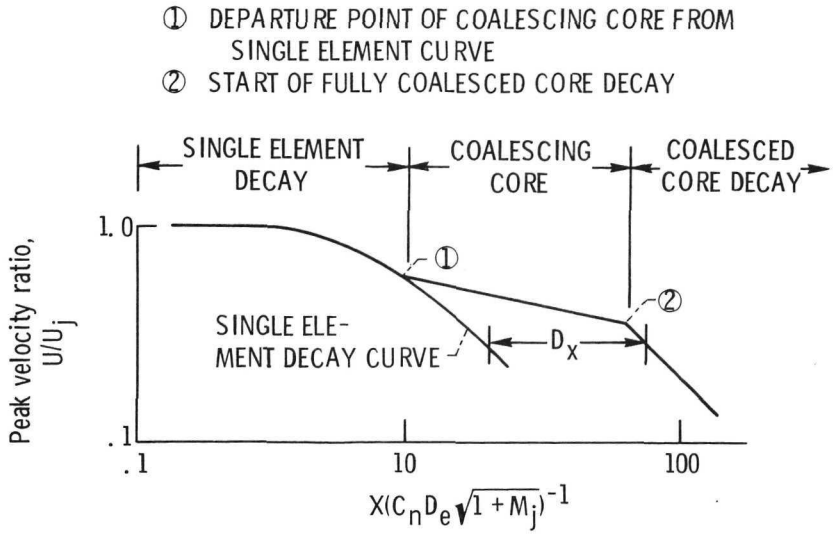

Figure 8. - Significant mixed-flow regimes for multi-element nozzles.

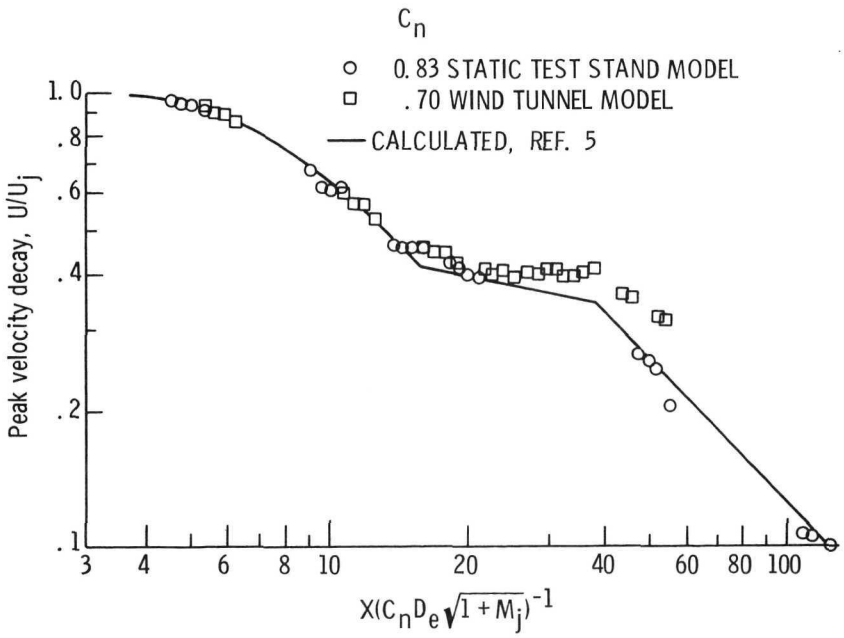

Figure 9. - Velocity decay for mixer nozzle, $M_0 = 0$.

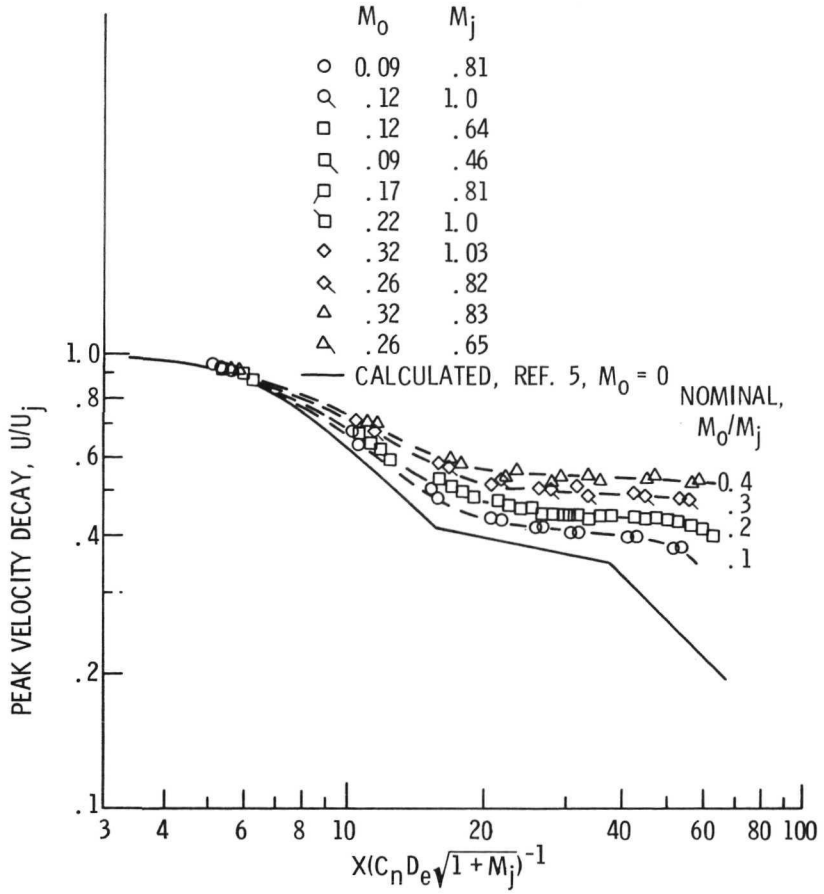

Figure 10. - Velocity decay for mixer nozzle with forward velocity. C_n, 0.7.

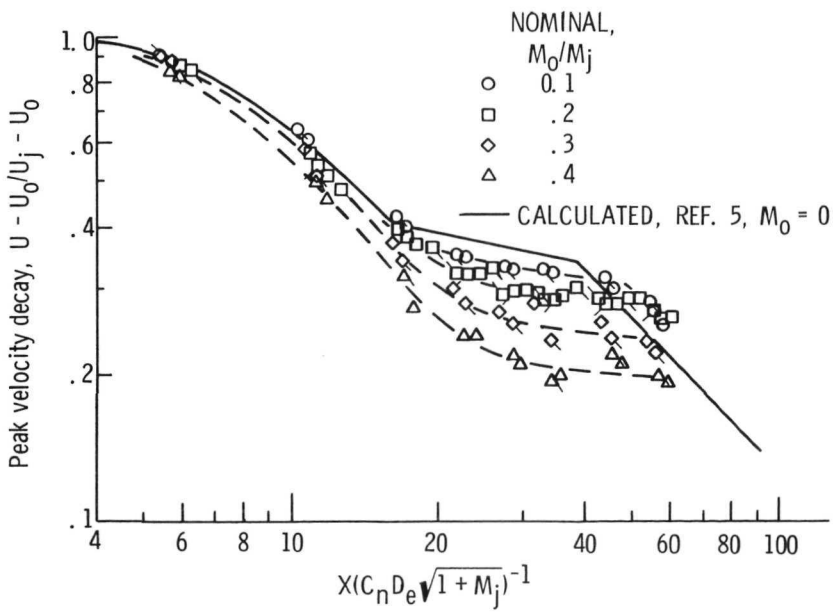

Figure 11. - Delta velocity decay for mixer nozzle with forward velocity.

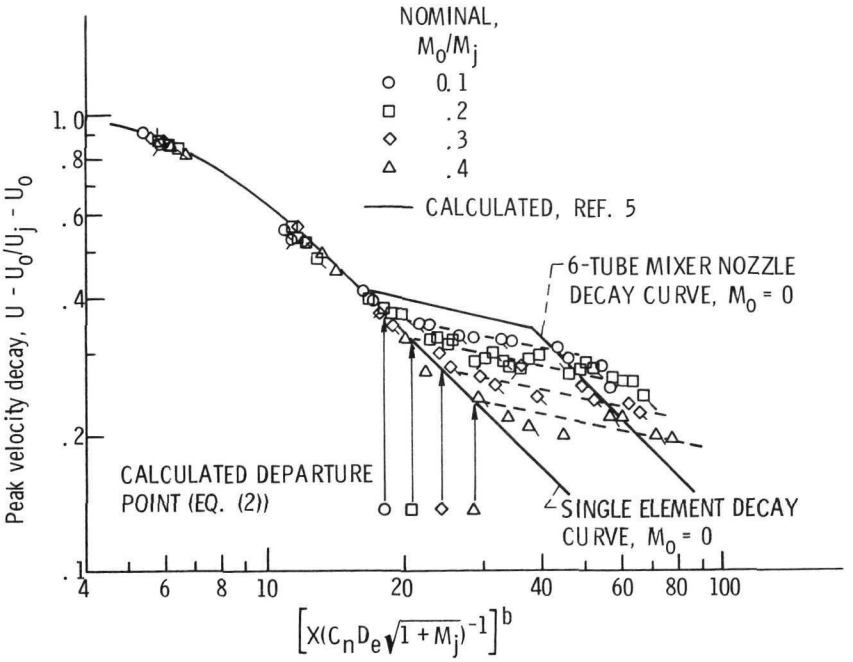

Figure 12. - Correlation of delta velocity decay for mixer nozzle.

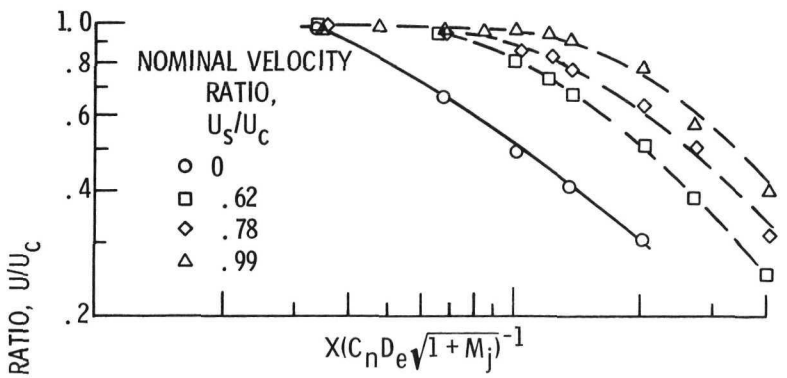

(a) EFFECT OF SECONDARY FLOW RATE ON BYPASS NOZZLE VELOCITY DECAY. C_n, 0.5.

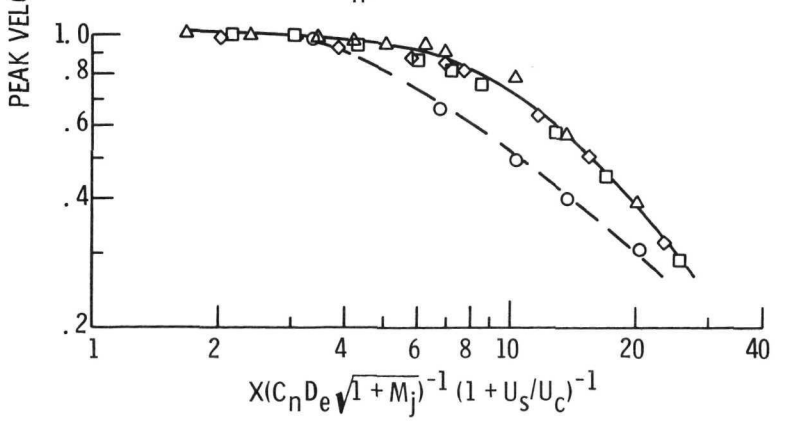

(b) NORMALIZATION OF VELOCITY DECAY FOR BYPASS NOZZLE.

Figure 13. - Peak velocity decay for bypass-type nozzle.

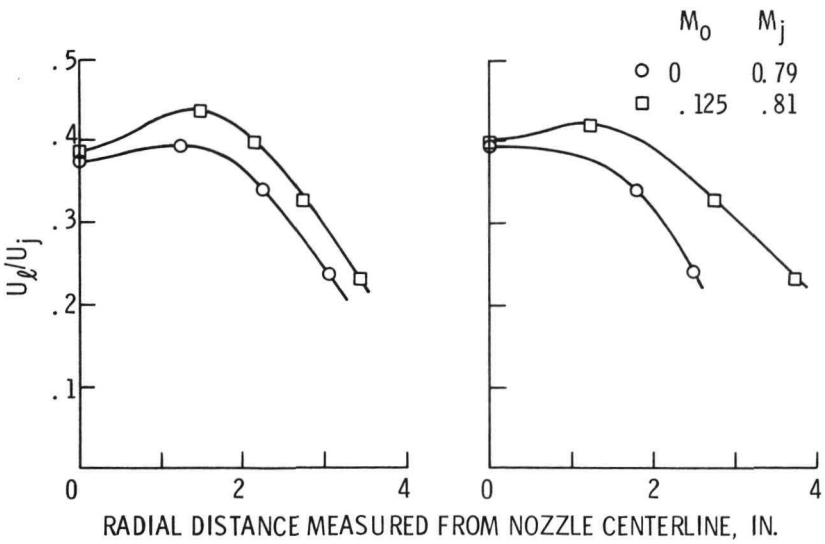

(a) AXIAL LOCATION, X = 20-IN. (b) AXIAL LOCATION, X = 25-IN.

Figure 14. - Typical radial velocity profiles for mixer nozzle near departure point of coalescing core decay curve from single element decay curve.

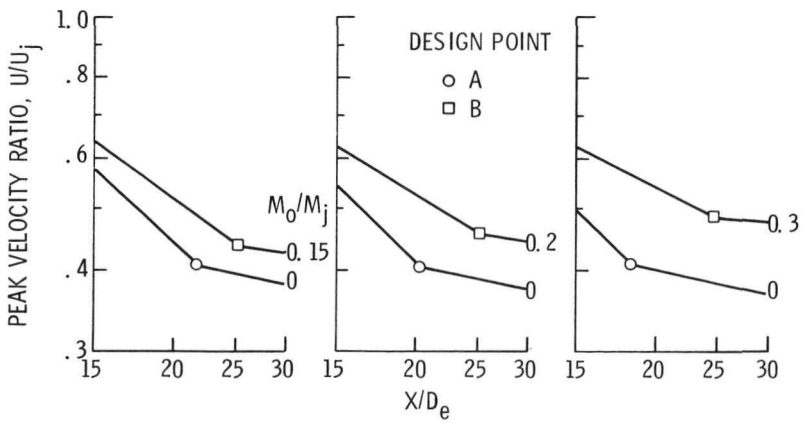

(a) BYPASS RATIO, 6; M_j, 0.78. (b) BYPASS RATIO, 15; M_j, 0.58. (c) BYPASS RATIO, 25; M_j, 0.4.

Figure 15. - Predicted velocity decay curves for 6-tube mixer nozzle used with possible EBF propulsion systems. Nominal M_0, 0.12.